Pergamon

Geochimica et Cosmochimica Acta, Vol. 59, No. 19, pp. 3953–3959, 1995

0016-7037/95 $9.50 + .00

0016-7037(95)00258-8

Synthetic fluid inclusions: XIII. Experimental determination of *PVT* properties in the system H_2O + 40 wt% NaCl + 5 mol% CO_2 at elevated temperature and pressure*

C. SCHMIDT, K. M. ROSSO, and R. J. BODNAR

Fluids Research Laboratory, Department of Geological Sciences, Virginia Polytechnic Institute and State University, Blacksburg, VA 24061-0420, USA

(*Received October* 5, 1994; *accepted in revised form April* 5, 1995)

Abstract—The location of the liquid + vapor → liquid phase boundary and the *P-T* slopes of iso-*Th* lines were determined for a constant composition of 40 ± 0.1 wt% NaCl and 5 ± 0.15 mol% CO_2 (both relative to H_2O) at high density. Synthetic fluid inclusions with this composition were formed in cold-seal pressure vessels at pressures of 2 and 4 kbar and temperatures between 350° and 700°C. The inclusions were analyzed on a gas-flow heating/cooling stage to determine the temperatures of halite dissolution [$Tm_{(H+L+V\rightarrow L+V)}$] and total homogenization [$Th_{(L+V\rightarrow L)}$].

Addition of 40 wt% NaCl to an aqueous solution containing 5 mol% CO_2 causes a significant shift of the liquid + vapor → liquid boundary towards higher pressures. The slopes of the iso-*Th* lines decrease from 29.5 bars/°C for $Th_{(L-V\rightarrow L)}$ of 400°C, to 6.4 bars/°C for $Th_{(L+V\rightarrow L)}$ = 600°C. Addition of 5 mol% CO_2 to an aqueous solution containing 40 wt% NaCl results in halite dissolution temperatures that are slightly higher ($Tm_{(H+L+V\rightarrow L+V)} \approx 332$°C) than the literature value of 323°C for the vapor-saturated liquidus of an H_2O-40 wt% NaCl mixture.

Calculated molar volumes for 40 wt% NaCl + 5 mol% CO_2 solutions at 2 and 4 kbar show trends that are similar to those of other compositions in the ternary system H_2O-CO_2-NaCl at the same pressures and temperatures. In the *P-T* range of this study, all excess volumes are negative and lie between the values for the compositions H_2O-5 mol% CO_2 and H_2O-40 wt% NaCl.

1. INTRODUCTION

The system H_2O-NaCl-CO_2 is one of the most important fluid systems in geochemistry. Fluid inclusions approximated by this ternary system are abundant in metamorphic rocks of all grades (except perhaps very low grade rocks and eclogites), particularly if carbonates were involved in the metamorphic process. Carbon dioxide concentrations of metamorphic fluids vary over wide ranges and the salinity can exceed 50 eq. wt% NaCl (Roedder, 1984). Furthermore, stability fields in *P-T* space of reactions which involve H_2O and CO_2 may be shifted considerably owing to the fact that addition of NaCl to a H_2O-CO_2 mixture significantly affects the fugacities of both H_2O and CO_2 (Bowers and Helgeson, 1983). Inclusions containing predominantly aqueous salt solutions and CO_2 are also frequently reported from igneous rocks, especially granites, pegmatites, carbonatites, and alkaline rocks, and in many hydrothermal deposits, e.g., Sn-W vein deposits, greisens, skarns, and other replacement deposits (Roedder, 1984).

Owing to various experimental difficulties, few studies have been conducted to determine the *PVTX* properties of H_2O-NaCl-CO_2 mixtures at high temperatures and pressures. In fact, the only extensive dataset was given by Gehrig (1980) for the pseudobinary H_2O-CO_2-6 wt% NaCl for pressures up to 3 kbar and temperatures between 150°C and 500°C, along with some data for 10 and 20 wt% NaCl relative to H_2O. Kotelnikov and Kotelnikova (1990), Frantz et al. (1992), Johnson (1992), and Shmulovich and Plyasunova (1993) utilized synthetic fluid inclusion techniques to determine liquid-vapor immiscibility limits, a few lines of equal homogenization temperature (iso-*Th* lines) and isochores. Joyce and Holloway (1993) measured the activity of H_2O in the ternary mixture at 850°C and 2 kbar, and at 700°C and 5 and 6 kbar. Data for NaCl-rich compositions are scarce. However, Chou (1988) determined the halite liquidus temperature in H_2O-CO_2-NaCl mixtures at 2 kbar using differential thermal analysis.

Based on experimental results, mainly those of Gehrig (1980), and on theoretical considerations, Bowers and Helgeson (1983) presented a modified Redlich-Kwong equation of state, which is applicable over restricted ranges of pressures, temperatures, and salinities. Brown and Lamb (1989) approximated isochore locations by assuming ideal geometrical mixing between H_2O-NaCl and CO_2 as endmembers.

In this study, synthetic fluid inclusions are used in conjunction with Raman spectroscopy to obtain molar volumes and excess volumes for an aqueous solution of 40 wt% NaCl and 5 mol% CO_2, both relative to water, for temperatures between 350° and 700°C and pressures of 2 and 4 kbar. Furthermore, the slopes of iso-*Th* lines were calculated from microthermometric data and the liquid + vapor → liquid phase boundary location in *P-T* space was estimated.

2. DETERMINATION OF SOLVUS AND ISO-*Th* LINES

2.1. Methodology

The synthetic fluid inclusion technique has been described in detail by Bodnar and Sterner (1987) and Sterner and Bodnar (1991); therefore, only the general procedure and experimental aspects specific to this study are reported here. Platinum capsules were loaded with a fixed composition of 40 ± 0.1 wt% NaCl and 5 ± 0.15 mol% CO_2,

* Presented at the fifth biennial Pan-American Conference on Research on Fluid Inclusions (PACROFI V) held May 19–21, 1994, at the Instituto de Investigaciones Electricas in Cuernavaca, Morelos, Mexico.

both relative to water, and a prefractured quartz core, and subsequently sealed. The loading order of the starting materials was NaCl first, then silver oxalate in an amount adjusted to the NaCl weight, then H_2O was added until the desired salinity was attained, and finally the quartz core was placed into the capsule. In earlier runs, silica gel was added to promote the fracture healing process. However, we found that this resulted in water/NaCl ratios that were too high in some cases. Because the loading procedure took so long for each capsule (up to 1 hr), it is assumed that the silica gel adsorbed water from the atmosphere during the loading process, even though the silica gel was thoroughly dried before the loading process began. Therefore, these samples were discarded and silica gel was not used during later experiments reported here. Silver oxalate ($Ag_2C_2O_4$) rather than oxalic acid dihydrate was preferred as the CO_2 source because of a better control of the actual CO_2 amount and to avoid the problem of possible significant hydrogen concentrations in the synthetic fluid inclusions formed at relatively low temperatures. The CO_2 yield of the silver oxalate was checked before the experiments by decomposing known amounts of $Ag_2C_2O_4$ in sealed Pt capsules and measuring the weight loss after puncturing the capsule. The yield averaged 99.5 ± 0.2 wt%. Puncturing/weight loss after the runs generally gave apparent CO_2 yield values up to two percent higher than the prerun calibration values, i.e., up to 101.5% yield. This error reflects loss of some water by evaporation during the puncturing/weight loss analysis. The deviation of the actual CO_2 concentration from the desired value of 5 mol% relative to H_2O reached as much as +0.12 mol%, due to the difficulty of accurately adding small amounts of the two solids (NaCl and silver oxalate) during the loading process. The magnitude of compositional error for the salinity is less than ±0.2 wt% NaCl. The compositional uncertainty resulting from weighing silver oxalate, sodium chloride, and H_2O generally yields results within 1% of the actual value.

The synthetic fluid inclusions were formed by healing fractures in quartz cores in externally heated cold-seal pressure vessels at temperatures between 350° and 700°C and pressures of 2 and 4 kbar. Before the capsule equilibrated at the final temperature and pressure, the pressure was cycled several times at pressures above the solvus to avoid premature fracture healing and to promote compositional homogeneity of the fluid inclusions. Run durations were chosen according to the formation temperatures (Tf): 5 days for $Tf \geq 600$°C, 1–2 weeks for Tf between 500° and 600°C, and 3–6 weeks for $Tf < 500$°C. After the experiment was completed, the pressure vessel was cooled approximately isochorically. Using conservative estimates, the uncertainty in experimental pressure and temperature are estimated to be ±1% and ±0.5%, respectively. According to Sterner and Bodnar (1991), the molar volume error resulting from all experimental variables is less than about ±1%.

An additional potential error results from pressure leaks during the runs, particularly at high pressures. Owing to the laboratory design, the pressure could only be measured at the beginning and end of each experiment. Moreover, the method used to test the pressure at the end of the run has poor precision (± a few hundred bars) and could only be used to confirm major pressure leaks. As an additional means of documenting that the pressure in the bombs did not change during the experiments, capsules containing prefractured quartz and pure water were placed in the same pressure vessel as each of the H_2O-CO_2-NaCl capsules. Because the PVT properties of H_2O are known very accurately over the entire P-T range of our experiments, the homogenization temperature corresponding to the P-T conditions at the beginning of the experiment could be calculated. If the pressure (and temperature) did not change during the run, the iso-Th line corresponding to the homogenization temperature of these pure H_2O inclusions would intersect the P-T corresponding to the formation conditions. Samples that did not satisfy this condition were discarded.

After the runs, the samples were cut into small disks, polished, and examined petrographically. At room temperature, the inclusions contained aqueous liquid, halite, and CO_2 vapor. A liquid CO_2 phase was sometimes visible, particularly in large inclusions in samples having formation temperatures less than 600°C. Most inclusions also contained a small black opaque phase, which is probably silver (e.g., Diamond, 1992). In all samples, the fluid inclusions formed in the one-phase (liquid) field, as indicated by the constant relative phase volume proportions at room temperature.

In order to determine the temperatures of the relevant phase changes, the inclusions were analyzed on a gas-flow heating/cooling stage. The stage was calibrated at the triple point and the critical point of water using a synthetic fluid inclusion standard (Sterner and Bodnar, 1984). An additional calibration point for temperatures above 374.1°C was obtained by measuring the quartz α-β transition temperature of the samples. The accuracy of the measurements is better than ±2 degrees Celsius for temperatures less than 400°C, but decreases to about ±5 degrees Celsius above 500°C.

Temperatures of the following important phase transitions were determined during microthermometry: (1) the homogenization temperature of the CO_2-rich phases [$Th(CO_2)$], (2) the dissolution temperature of halite in the presence of liquid and vapor [$Tm_{(H+L+V\rightarrow L+V)}$], and (3) the total liquid-vapor homogenization temperature [$Th_{(L+V\rightarrow L)}$]. A typical heating run showing these phase changes is illustrated in Fig. 1. Table 1 summarizes the experimental conditions and the microthermometric and Raman-spectroscopic data obtained during this study.

The consistency of halite dissolution temperatures was used to check for compositional homogeneity. For most samples, the deviation of individual $Tm_{(H+L+V\rightarrow L+V)}$ values from the average was less than 2 degrees Celsius. Only samples having formation temperatures above 600°C showed occasionally larger deviations. If the $Tm_{(H+L+V\rightarrow L+V)}$ values varied by more than 4°C from the average, the sample was not used in this study.

Errors in $Th_{(L+V\rightarrow L)}$ are mainly the result of stretching of the inclusions during heating (e.g., Bodnar et al., 1989), owing to the high internal pressures, and from residual silver from the decomposition of silver oxalate used to generate CO_2. The uncertainties in $Th_{(L+V\rightarrow L)}$ attributed to stretching of the inclusions during the heating runs are largest for $Th_{(L+V\rightarrow L)}$ less than 400°C and greater than about 573°C (the quartz α-β transition temperature). At total homogenization temperatures less than about 550° to 600°C, no significant differences in $Th_{(L+V\rightarrow L)}$ were found between inclusions containing an opaque phase, presumably silver, and inclusions which did not contain this phase. Thus, silver from the silver oxalate only appears to be a problem for experimental conditions resulting in $Th_{(L+V\rightarrow L)}$ greater than about 550°C. Below this temperature, the solubility of silver is presumably too low to have a measureable effect on the homogenization behavior.

To determine the slopes of the iso-Th lines, the formation temperatures were regressed as a function of $Th_{(L+V\rightarrow L)}$ for each isobar using a least-squares technique. The iso-Th lines were then calculated by solving these two regression equations for the same Th value to obtain the formation temperatures corresponding to that homogeniza-

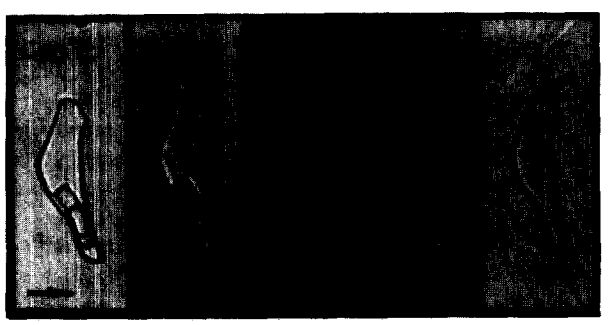

FIG. 1. Heating run on a synthetic H_2O-CO_2-NaCl inclusion having a composition of 5 mol% CO_2 and 40 wt% NaCl and formed at 500°C and 4 kbar. At −10°C, the inclusion contains a halite crystal, a CO_2-rich vapor bubble, liquid CO_2, and an aqueous phase saturated in carbon dioxide and NaCl. During heating the liquid CO_2 phase shrinks and disappears at 28.5°C, leaving CO_2 vapor, halite, and aqueous solution in the inclusion at 30°C. With continued heating, both halite and vapor become smaller and the halite crystal dissolves at 335°C. Due to the high internal pressure, the inclusion decrepitated at about 340°C. The total homogenization temperature of smaller inclusions in the same sample is 411°C. Scale bar equals 10 micrometers.

Table 1. Experimental conditions, microthermometric and Raman spectroscopic data for synthetic fluid inclusions having a composition of 40±0.1 wt% NaCl and 5±0.15 mole% CO_2, both relative to water

Tf	Pf	Salinity	Mole% CO_2	Th(L+V→L) (average)	Th(L+V→L) (range)	n	Tm(H+L+V→L+V) (average)	Tm(H+L+V→L+V) (range)	n	d(CO_2), MT, max	d(CO_2), RS, ave	d(CO_2), RS, range	n
400	2.0	39.99	4.98	395	391-398.5	7	332.4	330.0 - 333.6	8	0.271	n.d.		
450	2.0	40.05	4.97	434		1	334.1	333.0 - 336.7	9	0.235	0.292	0.269 - 0.321	6
450	2.0	40.00	4.97	432	423 - 441	5	333.8	331.5 - 335.6	11	0.208	n.d.		
500	2.0	39.99	4.96	471.5	467.2 - 475.7	8	331.5	330.0 - 334.4	11	0.224	0.248	0.225 - 0.273	4
550	2.0	40.03	4.99	509.0	506.4 - 511.4	12	337.6	336.9 - 338.3	10	0.207	0.230	0.213 - 0.261	6
600	2.0	39.98	5.12	574.8	573.5 - 576.1	7	338.3	336.6 - 340.0	10	0.167	0.213	0.185 - 0.233	10
625	2.0	40.02	4.95	582.9	579.3 - 586.1	10	337.8	337.1 - 338.7	12	0.163	0.200	0.181 - 0.229	9
650	2.0	40.01	5.00	596.7	591.8 - 601.3	7	337.6	334.4 - 341.5	13	0.162	n.d.		
700	2.0	40.00	4.96	625.4	617 - 630.5	7	339.0	337.0 - 340.3	8	0.155	0.178	0.137 - 0.221	4
350	4.0	40.02	5.05	345 ?	≈341 - 345	2	≈ 332		1	0.635	0.62 ?		1
400	4.0	39.96	5.02	371.5	363 - 378.5	8	333.7	332.1 - 335.1	6	n.d.	n.d.		
450	4.0	40.06	4.93	392.0	388.1 - 393.2	10	334.7	333.7 - 336.9	11	0.331	0.409	0.394 - 0.418	4
500	4.0	40.02	4.97	410.8	407.5 - 413.3	11	334.5	333.8 - 335.4	11	0.298	0.368	0.341 - 0.402	20
550	4.0	40.04	4.98	428.1	424.9 - 431.6	11	334.0	332.8 - 334.6	11	0.289	0.325	0.289 - 0.349	10
600	4.0	40.04	5.01	449.9	446.5 - 452.4	20	335.9	334.0 - 337.8	20	0.258	0.274	0.265 - 0.277	4
650	4.0	40.05	5.00	475.8	474.2 - 477.3	12	341.4	340.7 - 342.3	12	0.23	0.237	0.232 - 0.241	3
650	4.0	40.08	4.97	471.7	470.4 - 472.6	12	336.6	335.4 - 338.0	11	0.231	n.d.		
700	4.0	40.04	5.01	484.2	479.0 - 489.4	14	336.4	333.9 - 338.2	14	0.23	0.218	0.197 - 0.241	6

Tf = formation temperature (°C); Pf = formation pressure (kbar); Salinity = NaCl concentration of the solution in weight percent relative to H_2O; Mole% CO_2 = carbon dioxide concentration in mole percent relative to H_2O; Th(L+V→L) (average) = average liquid-vapor homogenization temperature (homogenization to the liquid, aqueous phase) (°C); Th(L+V→L) (range) = the range in measured Th(L+V→L) (°C); n = number of measured inclusions; Tm(H+L+V→L+V) (average) = average halite dissolution temperature in presence of liquid and vapor (°C); Tm(H+L+V→L+V) (range) = the range in measured Tm(H+L+V→L+V) (°C); d(CO_2), MT, max = maximum CO_2 density obtained from microthermometric measurements (g·cm^{-3}); d(CO_2), RS, ave = average CO_2 density at 32 °C calculated from the Raman spectroscopic CO_2 peak separation (g·cm^{-3}); d(CO_2), RS, range = range in Raman-spectroscopically obtained CO_2 densities at 32 °C (g·cm^{-3}); n.d. = not determined.

tion temperature. A linear fit to these *P-T* data points was used to determine the iso-*Th* line. The pressure of the liquid + vapor → liquid phase boundary was obtained by extrapolating the iso-*Th* lines to the total homogenization temperature corresponding to that line.

2.2. Results

A *P-T* projection of iso-*Th* lines and the estimated location of a portion of the H_2O-5 mol% CO_2-40 wt% NaCl bubble-point curve is shown in Fig. 2. Although isochore plots are more common in the literature, it was preferred here to present the data as a function of homogenization temperature instead of molar volume or density. Iso-*Th* lines are more convenient for fluid inclusion studies and avoid errors (these will be discussed later) associated with the bulk density calculations. In the investigated temperature range, the slopes of the iso-*Th* lines change considerably from 29.5 bar/°C for a $Th_{(L+V\rightarrow L)}$ of 400°C to 6.4 bar/°C for $Th_{(L+V\rightarrow L)}$ = 600°C. Addition of 5 mol% CO_2 to an aqueous 40 wt% NaCl solution results in a significant steepening of the lines of constant liquid-vapor homogenization temperature at $Th_{(L+V\rightarrow L)}$ less than about 600°C.

The obtained portion of the H_2O-5 mol% CO_2-40 wt% NaCl liquid + vapor → liquid solvus is compared to the *P-T* location of the liquid-vapor immiscibility boundary for the composition H_2O-5 mol% CO_2 (Takenouchi and Kennedy, 1964) and the liquid + vapor → liquid phase boundary of H_2O-5 mol% CO_2-20 wt% NaCl (Gehrig, 1980) in Fig. 3. Also shown is the liquid-vapor curve for a 40 wt% NaCl solution (Bodnar, 1994). As expected, the addition of NaCl to a H_2O-CO_2 mixture raises the pressure of the liquid + vapor → liquid phase boundary significantly. In contrast to the curves for 6, 10, and 20 wt% NaCl determined by Gehrig (1980),

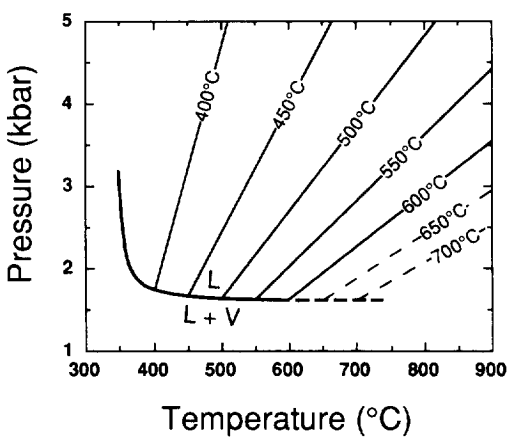

FIG. 2. Iso-*Th* lines (homogenization to the liquid phase) and the liquid + vapor → liquid phase boundary for the composition H_2O-5 mol% CO_2-40 wt% NaCl. "L" refers to liquid; "V" refers to vapor.

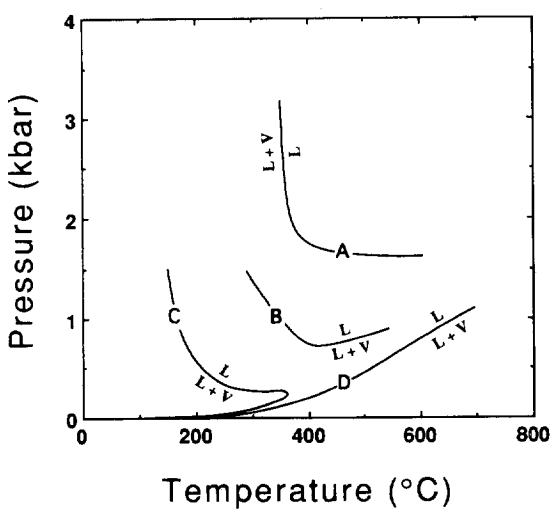

FIG. 3. *P-T* projection of liquid-vapor immiscibility boundaries for the compositions H_2O-5 mol% CO_2 (curve C, from Takenouchi and Kennedy, 1964), H_2O-5 mol% CO_2-20 wt% NaCl (curve B, from Gehrig, 1980) and H_2O-5 mol% CO_2-40 wt% NaCl (this study, curve A). The liquid-vapor curve for H_2O-40 wt% NaCl (line D) is from Bodnar (1994).

Table 2. Calculated volumetric properties of H_2O - 40 wt% NaCl - 5 mole% CO_2 at elevated temperatures and pressures

Tf	Pf	d(CO_2) at 32 °C	P(CO_2) at 32 °C	V(bulk) at 32 °C, P(CO_2)	V(bulk) at Tf, Pf	V_{ID} at Tf, Pf	V_{EX} at Tf, Pf
450	2.0	0.287	73.2	24.21	24.55	26.27	-1.72
500	2.0	0.256	71.2	24.91	25.35	27.84	-2.49
550	2.0	0.230	69.0	25.64	26.21	29.64	-3.43
600	2.0	0.209	66.6	26.37	27.16	31.68	-4.52
650	2.0	0.192	64.3	27.10	28.25	33.92	-5.67
700	2.0	0.176	61.9	27.85	29.04	36.34	-7.3
350	4.0	0.629	124.8	21.13	21.19	21.56	-0.37
400	4.0	0.513	90.3	21.69	21.80	22.24	-0.44
450	4.0	0.429	80.2	22.32	22.49	22.98	-0.49
500	4.0	0.365	76.6	22.99	23.24	23.78	-0.54
550	4.0	0.316	74.6	23.69	24.03	24.65	-0.62
600	4.0	0.276	72.6	24.44	24.91	25.55	-0.64
650	4.0	0.245	70.4	25.20	25.88	26.50	-0.62
700	4.0	0.218	67.7	26.04	27.07	27.50	-0.43

Tf = formation temperature (°C); Pf = formation pressure (kbar); d(CO_2) at 32°C = smoothed densities of the carbonic phase at 32°C, based on the Raman spectroscopic data ($g \cdot cm^{-3}$); P(CO_2) at 32°C = pressure of the carbonic phase at 32 °C (bar); V(bulk) at 32°C, P(CO_2) = bulk molar volume at 32°C and corresponding internal pressure ($cm^3 \cdot mole^{-1}$); V(bulk) at Tf, Pf = bulk molar volume at formation temperature and pressure ($cm^3 \cdot mole^{-1}$); V_{ID} at Tf, Pf = ideal molar volume at formation temperature and pressure ($cm^3 \cdot mole^{-1}$); V_{EX} at Tf, Pf = excess molar volume at formation temperature and pressure ($cm^3 \cdot mole^{-1}$)

the calculated liquid + vapor → liquid solvus of the ternary composition investigated in this study does not show a pressure minimum. The lack of a pressure minimum in the bubble-point curve from this study may be more apparent than real, and reflects our lack of data in the higher temperature region where the pressure is expected to increase.

Halite dissolution temperatures in CO_2-bearing aqueous solutions of this study (see Table 1) are slightly, but consistently, elevated compared to the $Tm_{(H+L+V \rightarrow L+V)}$ = 323°C for the vapor-saturated liquidus (liquid + vapor + halite) of H_2O-40 wt% NaCl obtained by Bodnar (1994). Additionally, $Tm_{(H+L+V \rightarrow L+V)}$ increases somewhat with increasing $Th_{(L+V \rightarrow L)}$ (Table 1). It remains to be determined whether the elevated $Tm_{(H+L+V \rightarrow L+V)}$ is related to the loss of water from the aqueous liquid to the carbonic phase, as suggested by the relationship between $Tm_{(H+L+V \rightarrow L+V)}$ and $Th_{(L+V \rightarrow L)}$ (Chou, 1987), or is caused by the presence of dissolved AgCl and/or CO_2 in the aqueous phase, or both. However, the effect is small in any case. Assuming that the increased $Tm_{(H+L+V \rightarrow L+V)}$ is not a result of AgCl in solution, the temperature of the vapor-saturated liquidus is approximately 332°C for the investigated ternary composition.

3. DETERMINATION OF CO_2 DENSITIES AND BULK MOLAR VOLUME CALCULATION

3.1. Raman Spectroscopic Determination of CO_2 Densities

In all samples, except the one formed at 350°C and 4 kbar, CO_2 homogenization occurred to the vapor phase. As pointed out by Sterner and Bodnar (1991), microthermometric measurements will underestimate the $Th(CO_2)$ of such inclusions, owing to the difficulty in observing the evaporation of the last liquid CO_2. This will result in CO_2 densities that are too low and, consequently, calculated molar volumes that are too large. Microthermometric measurements are also subject to significant errors if the CO_2 density is close to the critical density of CO_2, where a large change in density occurs over a small change in $Th(CO_2)$. To eliminate errors introduced by determining CO_2 densities from microthermometric data, a Raman spectroscopic method was used to determine the CO_2 densities.

Raman spectra of the CO_2 vapor phase were obtained using a Dilor XY spectrometer, equipped with a CCD detector (256 × 1024 element array), microscope, and an 80× objective lens. The 514.5 nm line of an Ar^+ laser provided the excitation energy. The scattered light was analyzed using a 0.64 m focal-length spectrometer in double subtractive mode. Spectra were collected using 750 mW laser power at the source and integration times ≥ 180 seconds. Entrance and exit slits were each set at 100 μm, which corresponds to 4.6 cm^{-1} spectral resolution. The spectrometer was regularly calibrated between analyses using a neon lamp and a mercury line to check the absolute wavenumber alignment and to correct for any frequency offsets. This offset was found to be small and linear but showed some variability over long integration times.

The samples were placed in a temperature-controlled, Joule-Thompson optical stage (Rosso and Bodnar, 1995) and were analyzed at 32°C in order to insure that the vapor phase was homogeneous. At this temperature, the partial pressure of H_2O [$p(H_2O)$] is 0.05 bar for pure H_2O (Haar et al., 1984). However, in aqueous inclusions containing salts or other dissolved solutes, in this case NaCl at saturation and CO_2, $p(H_2O)$ is expected to be less than that for pure water. Thus the vapor phase can reasonably be assumed to consist of essentially pure CO_2.

Rosso and Bodnar (1995) have shown that the density of CO_2 in fluid inclusions can be calculated with reasonable accuracy based on the separation of the ν_1-$2\nu_2$ Fermi diad in the Raman spectrum of CO_2. The spectra were analyzed using a maximum likelihood fitting program. Individual CO_2 band shapes were least-squares fit to minimize errors and maximize precision in the determination of the band separation (X) of the ν_1-$2\nu_2$ diad. The values of X were converted to CO_2 density [$d(CO_2)$] using the relationships given by Rosso and Bodnar (1995). Table 1 lists the obtained average CO_2 densities calculated from the CO_2 peak separation. The densities

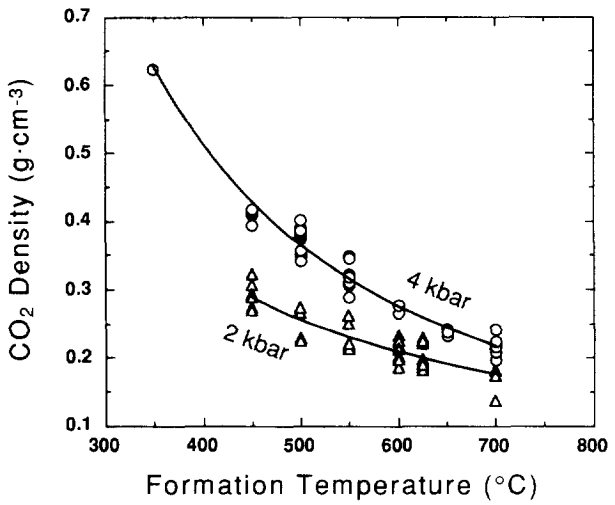

FIG. 4. Densities of the CO_2 phase at 32°C for synthetic fluid inclusions having a constant composition of 5 mol% CO_2 and 40 wt% NaCl, both relative to H_2O, plotted as a function of formation temperature along the 2 and 4 kbar isobars. The densities were calculated from Raman spectroscopic data as described in the text.

of the carbonic phase were, in turn, converted to CO_2 pressure [$P(CO_2)$] using the equations of state of Duschek et al. (1990) for low densities (≤ 0.2 g·cm^{-3}) and Bottinga and Richet (1981) for densities > 0.2 g·cm^{-3} (see Table 2). This pressure was taken to be equal to the inclusion internal pressure. The estimated standard error in $d(CO_2)$ is approximately 0.02 g·cm^{-3}. Thus, for low density inclusions, the uncertainty in $P(CO_2)$ for a single value is significant. For example, for a $d(CO_2)$ of 0.08 g·cm^{-3}, the uncertainty in the calculated $P(CO_2)$ amounts to about 17%. Therefore, the average of several analyses was used to minimize this problem. This proved to be somewhat difficult owing to the fact that inclusions with very large CO_2 bubbles were required to obtain high-quality spectra. This necessity limits the number of analyses, especially for samples having formation temperatures less than 500°C, due to the generally small size of such inclusions.

3.2. Calculation of Bulk Molar Volumes

The salinity of all samples was close to 40 wt% NaCl relative to water. The halite saturation point in these solutions was estimated using the equation for the NaCl-H_2O binary in Sterner et al. (1988) assuming that dissolved CO_2 has a negligible effect on halite solubility. This NaCl concentration was used to calculate the solubility of CO_2 and the density of the solution from the spectroscopically determined internal pressure at a temperature of 32°C. This was carried out according to the formulations given in Barton and Chou (1993) which are based on the data of Drummond (1981). These equations correct Henry's Law constants for deviations due to the nonideal behavior of CO_2. The results were combined with the known bulk composition to calculate the phase ratios and the bulk molar volumes of the fluids listed in Table 2. To relate the molar volumes at $P(CO_2)$ and 32°C to those at the temperature and pressure of formation, corrections were made for the slight nonisochoric behavior of the quartz host of the inclusions. These corrections were carried out following the procedure described by Sterner and Bodnar (1991), using the equation of state of quartz in Hosieni et al. (1985). The molar volumes at *Tf* and *Pf* calculated in this manner are given in Table 2.

3.3. Results and Discussion

Individual data points for the density of the carbonic phase as determined by Raman spectroscopy are plotted in Fig. 4 along the 2 and 4 kbar isobars as a function of formation temperature. The minimum standard deviation of $d(CO_2)$ is ± 0.02 g·cm^{-3} (Rosso and Bodnar, 1995). For a high-quality spectrum, a typical peak fitting error of 0.01 cm^{-1} results in a $d(CO_2)$ uncertainty of ± 0.008 g·cm^{-3}. The large scatter of the data in Fig. 4 is probably caused by the long integration (data-collection) times, which necessitate longer intervals between calibrations with the neon source. Those samples which showed homogenization to the vapor phase precluded an accurate microthermometric determination of $Th(CO_2)$. These measurements resulted in a consistent underestimation of the CO_2 density in the inclusions as compared to values determined by the Raman technique (Fig. 5). Raman spectroscopy proves to be more accurate than microthermometry for determining CO_2 densities in the range from about 0.55 to 0.2 g·cm^{-3}.

The calculated molar volumes of the H_2O-5 mol% CO_2-40 wt% NaCl solutions at 2 and 4 kbar are shown in Fig. 6 as a function of temperature, and compared to molar volumes of other compositions in the H_2O-CO_2-NaCl ternary. Using these molar volumes, excess volumes (V_{EX}) were calculated at formation temperature and pressure. The molar volume of H_2O at P and T was taken from Haar et al. (1984), that of CO_2 from Bottinga and Richet (1981) and that of NaCl, using metastable, supercooled liquid NaCl as the standard state, from Bodnar (1985). The results are given in Table 2. A plot

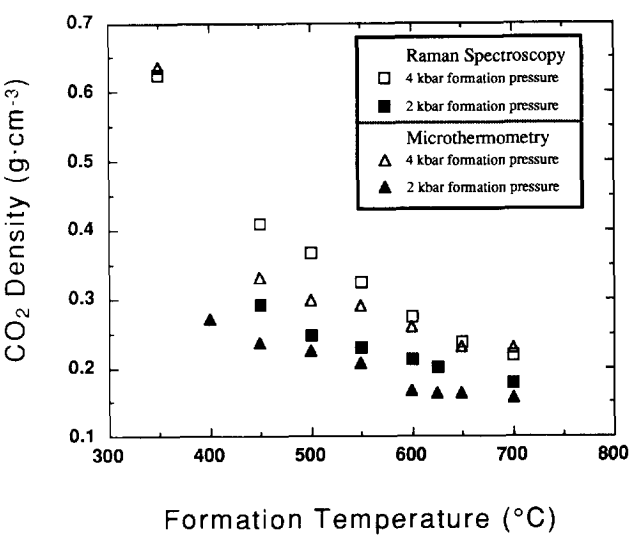

FIG. 5. Average CO_2 densities at 32°C determined by Raman spectroscopy (squares) compared to the maximum CO_2 density obtained from microthermometric analysis (triangles) of the same samples.

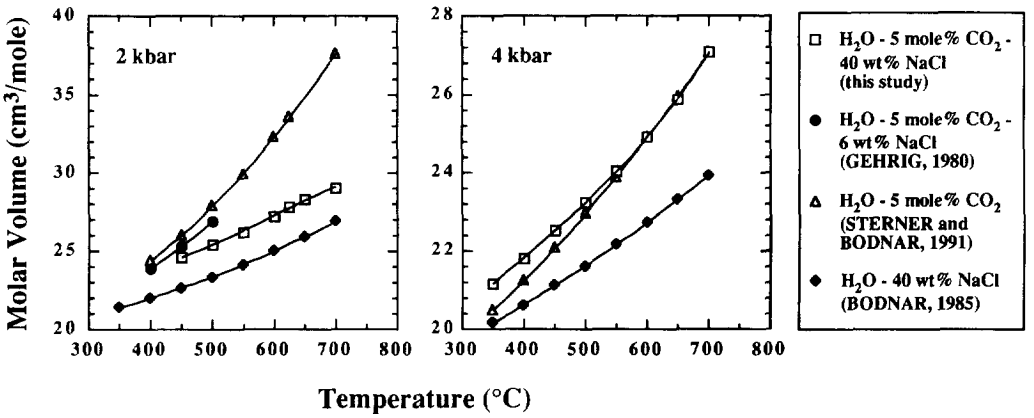

FIG. 6. Comparison of molar volumes for various compositions in the ternary system H_2O-CO_2-NaCl at 2 and 4 kbar pressure.

of excess volume versus formation temperature for compositions in the H_2O-CO_2-NaCl system (Fig. 7) confirms the observation of Gehrig (1980) and Gehrig et al. (1986) that addition of CO_2 to an aqueous sodium chloride solution results in less negative or positive V_{EX}. The calculated molar excess volumes are somewhat inconsistent for $Tf > 600$°C, which is most obvious at 4 kbar formation pressure, where the V_{EX} values become less negative with increasing temperature. This inconsistency could reflect the relatively large uncertainties associated with the Raman spectroscopic density determination or could be a result of small compositional heterogeneities in these samples (cf. Sterner, 1992), although this was only evidenced to a minor extent in the 650°C, 2 kbar and 700°C, 2 kbar runs.

4. SUMMARY

Using the synthetic fluid inclusion technique, the slopes of iso-*Th* lines and the location of the liquid + vapor → liquid solvus for an H_2O-40 wt% NaCl-5 mol% CO_2 solution were determined. The addition of 40 wt% NaCl to an H_2O-5 mol% CO_2 mixture causes a significant shift of the liquid + vapor → liquid curve towards higher pressures and indicates that immiscibility is likely to occur in medium-to-high grade metamorphic environments in which the fluids contain high concentrations of salts. The slopes of iso-*Th* lines decrease from 29.5 bars/°C for $Th_{(L+V\rightarrow L)}$ = 400°C, to 6.4 bars/°C for $Th_{(L+V\rightarrow L)}$ = 600°C. As previous workers have documented (Bodnar et al., 1985; Sterner and Bodnar, 1991), the temperature of homogenization to the vapor phase is difficult to determine accurately, resulting in large errors in densities calculated from Th measurements. To avoid this problem, the density of the CO_2 phase in inclusions from this study was calculated from the CO_2 pressure determined from Raman spectroscopic analysis of the inclusions. These data permit estimation of the molar volumes and excess molar volumes of H_2O-40 wt% NaCl-5 mol% CO_2 solutions over the approximate range 350° to 700°C and 2 to 4 kbars.

Acknowledgments—This research was sponsored by the Geosciences Program, Office of Basic Energy Sciences, US Department of Energy (DOE) under Grant DE-FG05-89ER14065 to RJB. The authors would like to thank David Hewitt, Frank Harrison, Sarah Beutner, John Mavrogenes, and Brenda Kutz for their support and assistance with various aspects of this study. Discussions and advice provided by S. Michael Sterner and Charles S. Oakes concerning experimental techniques are appreciated. Reviews of an earlier version of this man-

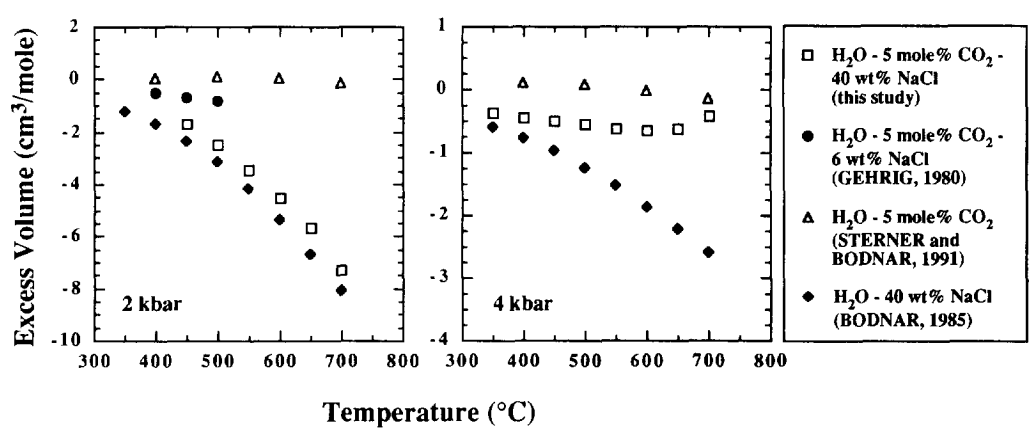

FIG. 7. Comparison of excess volumes for various compositions in the ternary system H_2O-CO_2-NaCl at 2 and 4 kbar pressure.

uscript by I-Ming Chou, Larryn Diamond, and Will Lamb clarified many aspects of the interpretation and presentation of the data.

Editorial handling: P. E. Brown

REFERENCES

Barton P. B. and Chou I-M. (1993) Calculation of the vapor-saturated liquidus for the NaCl-CO_2-H_2O system. *Geochim. Cosmochim. Acta* **57,** 2715–2723.

Bodnar R. J. (1985) Pressure-volume-temperature-composition (PVTX) properties of the system H_2O-NaCl at elevated temperatures and pressures. Unpubl. Ph.D. Dissertation, Penn. State Univ.

Bodnar R. J. (1994) Synthetic fluid inclusions: XII. The system H_2O-NaCl. Experimental determination of the halite liquidus and isochores for a 40 wt% NaCl solution. *Geochim. Cosmochim. Acta* **58,** 1053–1063.

Bodnar R. J. and Sterner S. M. (1987) Synthetic fluid inclusions. In *Hydrothermal Experimental Techniques* (ed. G. C. Ulmer and H. L. Barnes), pp. 423–457. Wiley.

Bodnar R. J., Burnham C. W., and Sterner S. M. (1985) Synthetic fluid inclusions in natural quartz. III. Determination of phase equilibrium properties in the system H_2O-NaCl to 1000°C and 1500 bars. *Geochim. Cosmochim. Acta* **49,** 1861–1873.

Bodnar R. J., Binns P. R., and Hall D. L. (1989) Synthetic fluid inclusions. VI. Quantitative evaluation of the decrepitation behavior of fluid inclusions in quartz at one atmosphere confining pressure. *J. Metam. Geol.* **7,** 229–242.

Bottinga Y. and Richet P. (1981) High pressure and temperature equation of state and calculation of the thermodynamic properties of gaseous carbon dioxide. *Amer. J. Sci.* **281,** 615–660.

Bowers T. S. and Helgeson H. C. (1983) Calculation of the thermodynamic and geochemical consequences of nonideal mixing in the system H_2O-CO_2-NaCl on phase relations in geologic systems: Equation of state for H_2O-CO_2-NaCl fluids at high pressures and temperatures. *Geochim. Cosmochim. Acta* **47,** 1247–1275.

Brown P. E. and Lamb W. M. (1989) P-V-T properties of fluids in the system $H_2O \pm CO_2 \pm$ NaCl: New graphical presentations and implications for fluid inclusion studies. *Geochim. Cosmochim. Acta* **53,** 1209–1221.

Chou I-M. (1987) Phase relations in the system NaCl-KCl-H_2O. III. Solubilities of halite in vapor-saturated liquids above 450°C and redetermination of the phase equilibrium properties in the system NaCl-H_2O to 1000°C and 1500 bars. *Geochim. Cosmochim. Acta* **51,** 1965–1975.

Chou I-M. (1988) Halite solubilities in supercritical carbon dioxide-water fluids. *GSA Abstr. Prog.* **20,** A76.

Diamond L. W. (1992) Stability of CO_2 clathrate hydrate + CO_2 liquid + CO_2 vapour + aqueous KCl-NaCl solutions: Experimental determination and application to salinity estimates of fluid inclusions. *Geochim. Cosmochim. Acta* **56,** 273–280.

Drummond S. E., Jr. (1981) Boiling and mixing of hydrothermal fluids: Chemical effects on mineral precipitation. Unpubl. Ph.D. Dissertation, Penn. State Univ.

Duschek W., Kleinrahm R., and Wagner W. (1990) Measurement and correlation of the (pressure, density, temperature) relation of carbon dioxide. I. The homogeneous gas and liquid regions in the temperature range from 217 K to 340 K at pressures up to 9 MPa. *J. Chem. Thermodyn.* **22,** 827–840.

Frantz J. D., Popp R. K., and Hoering T. C. (1992) The compositional limits of fluid immiscibility in the system H_2O-NaCl-CO_2 as determined with the use of synthetic fluid inclusions in conjunction with mass spectrometry. *Chem. Geol.* **98,** 237–255.

Gehrig M. (1980) Phasengleichgewichte und PVT-Daten ternärer Mischungen aus Wasser, Kohlendioxid und Natriumchlorid bis 3 kbar und 550°C. Doctoral dissertation, Univ. Karlsruhe.

Gehrig M., Lentz H., and Franck E. U. (1986) The system water-carbon dioxide-sodium chloride to 773 K and 300 MPa. *Ber. Bunsenges. Phys. Chemie* **90,** 525–533.

Haar L., Gallagher J. S., and Kell G. S. (1984) NBS/NRC Steam Tables: Thermodynamic and Transport Properties and Computer Programs for Vapor and Liquid States in SI Units. Hemisphere Publ. Co.

Hosieni K. R., Howald R. A., and Scanlon M. W. (1985) Thermodynamics of the lambda transition and the equation of state of quartz. *Amer. Mineral.* **70,** 782–793.

Johnson, E. L. (1992) An assessment of the accuracy of isochore location techniques for H_2O-CO_2-NaCl fluids at granulite facies pressure-temperature conditions. *Geochim. Cosmochim. Acta* **56,** 295–302.

Joyce D. B. and Holloway J. R. (1993) An experimental determination of the thermodynamic properties of H_2O-CO_2-NaCl fluids at high pressures and temperatures. *Geochim. Cosmochim. Acta* **57,** 733–746.

Kotelnikov A. R. and Kotelnikova Z. A. (1990) An experimental study of the phase state of the system H_2O-CO_2-NaCl using synthetic fluid inclusions in quartz. *Geokhimiya* **4,** 526–537 (in Russian).

Roedder E. (1984) *Fluid Inclusions. Rev. Mineral.* **12.**

Rosso K. M. and Bodnar R. J. (1995) Microthermometric and Raman spectroscopic detection limits of CO_2 in fluid inclusions and the Raman spectroscopic characterization of CO_2. *Geochim. Cosmochim. Acta* **59,** 3961–3975 (this issue).

Shmulovich K. I. and Plyasunova N. V. (1993) Phase equilibria in ternary systems formed by H_2O and CO_2 with $CaCl_2$ or NaCl at high *T* and *P*. *Geochem. Intl.* **30,** 53–71.

Sterner S. M. (1992) Synthetic fluid inclusions. XI. Notes on the application of synthetic fluid inclusions to high *P-T* experimental aqueous geochemistry. *Amer. Mineral.* **77,** 156–167.

Sterner S. M. and Bodnar R. J. (1984) Synthetic fluid inclusions in natural quartz. I. Compositional types synthesized and applications in experimental geochemistry. *Geochim. Cosmochim. Acta* **48,** 2659–2668.

Sterner S. M. and Bodnar R. J. (1991) Synthetic fluid inclusions. X: Experimental determination of *P-V-T-X* properties in the CO_2-H_2O system to 6 kb and 700°C. *Amer. J. Sci.* **291,** 1–54.

Sterner S. M., Hall D. L., and Bodnar R. J. (1988) Synthetic fluid inclusions. V. Solubility relations in the system NaCl-KCl-H_2O under vapor-saturated conditions. *Geochim. Cosmochim. Acta* **52,** 989–1005.

Takenouchi S. and Kennedy G. C. (1964) The binary system H_2O-CO_2 at high temperatures and pressures. *Amer. J. Sci.* **262,** 1055–1074.